JOURNAL OF MATERIALS SCIENCE 24 (1989) 4209–4219

Review
Solid state NMR: Applications in high performance ceramics

GALEN R. HATFIELD*
Washington Research Center, W. R. Grace & Co., 7379 Route 32, Columbia, MD 21044, USA
KEITH R. CARDUNER
Scientific Research Laboratory, Ford Motor Company, Dearborn, Michigan 48121, USA

Solid state NMR is a new analytical tool that has proven to be both powerful and versatile in the characterization of ceramic systems. In this paper, we review many of the recent applications of NMR in ceramics, with an emphasis on applied research. Since solid-state NMR is a relatively new approach, a brief introduction into the technique is provided. Examples are given to illustrate how NMR can be used to (1) identify both crystalline *and* amorphous phases, (2) quantitate both crystalline *and* amorphous phases, (3) determine the structure of both crystalline *and* amorphous phases, (4) probe local structural order and (5) study the chemistry of ceramic systems. These capabilities are demonstrated in a series of brief applications including (1) a study of structure in a new ceramic material ($LaSi_3N_5$), (2) accurate phase composition analyses on commercial Si_3N_4 powders, (3) determination of structure and curing mechanisms in amorphous SiC fibres, (4) investigation of dispersion aid mechanisms, (5) determination of structure in several SiAlON ceramics and (6) identification and quantitation of phases typically associated with the grain boundaries of Y_2O_3 sintered Si_3N_4.

1. Introduction

Solid state nuclear magnetic resonance (NMR) has become an established and powerful technique for probing the structure and chemistry of solid materials. Most of the applications to date have been in organic systems such as polymers and resins. This emphasis has been primarily due to historical reasons. Recently, however, NMR is finding new applications in solid inorganic systems including ceramics and ceramic composites. In these complex systems, NMR is capable of identifying both crystalline and amorphous phases, determining the structure of such phases and studying the chemistry of these phases at the atomic level. Aside from this versatility, NMR provides several unique advantages including the ability to study amorphous phase structure and the ability to observe a wide variety of nuclei.

The purpose of this manuscript is to review many of the recent applications of NMR to highly refractory ceramics, specifically Si_3N_4, SiC and related materials. The primary interest is in materials that show promise in high temperature, high strength applications of significant industrial value. The emphasis of this review is on applied research of high performance ceramics and is not a complete overview of the ceramics field. Since solid state NMR is a relatively new approach, some time will be spent introducing the technique. As this review demonstrates, NMR is expected to play a growing role in ceramics research.

2. Experimental details

Experiments carried out by the authors were performed on either a Chemagnetics CMX300, a Varian XL200 or a Bruker MSL300 NMR spectrometer. All spectra were acquired using standard single-pulse or cross-polarization techniques under magic-angle spinning (MAS) conditions. The details of these techniques have been well described elsewhere [1–5] and will not be repeated here. Pulse delays ranged from 2 sec to 1 h. The samples investigated include fibres, sintered bars, powders and slips. For details on the literature cited results, the reader is referred to the original texts.

3. Background

This section will highlight many of the general concepts used when studying ceramic samples by high resolution NMR. More complete reviews on the theory and practice of solid state NMR are available [1–5] and the reader is referred to these texts for greater detail.

3.1. The NMR concept

The most basic description of NMR begins with the concept of a nucleus as a spinning charged particle with an associated magnetic moment. The direction of this moment is random in the absence of any magnetic field. However, if the nucleus encounters a magnetic field, $\boldsymbol{H}_0$, its moment typically aligns itself either with or against $\boldsymbol{H}_0$. The higher energy state (against $\boldsymbol{H}_0$) is less populated than the lower energy state (with $\boldsymbol{H}_0$)

*Address to whom correspondence should be sent.

0022–2461/89 $03.00 + .12

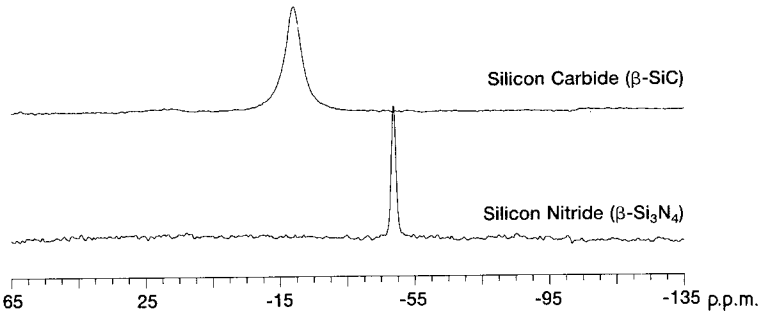

Figure 1 ^{29}Si NMR spectra of silicon carbide (β-SiC) and silicon nitride (β-Si_3N_4).

and it is possible to excite the nuclei by applying a "pulse" of energy. For a given nucleus in a given $\boldsymbol{H}_0$, the frequency of energy that causes this transition varies slightly depending on the electronic environment of that nucleus. The local electronic environment can "shield" or "deshield" the nucleus from the applied field, creating a "shift" in frequency. These differences, or shifts, are measured in the NMR experiment and called "chemical shifts".

3.2. The chemical shift

The chemical shift, then, is sensitive to the local environment around the nucleus. Different environments will give rise to different chemical shifts. This "environment" is largely determined by the bonding network surrounding the nucleus, including the identity of neighbouring atoms, the distances to those neighbours and the angles defined by their location.

As an illustration, consider two common ceramic materials, silicon carbide (SiC) and silicon nitride (Si_3N_4). In β-SiC, silicon nuclei are in a cubic site surrounded by carbon atoms. In β-Si_3N_4, however, they are in a tetrahedral site surrounded by nitrogen atoms. The different silicon environments should give rise to different ^{29}Si chemical shifts. In fact, the ^{29}Si NMR spectra of these materials reveals peaks at different shifts, as expected. As shown in Fig. 1, the ^{29}Si chemical shift of β-SiC is -18 p.p.m. and the shift of β-Si_3N_4 is -49 p.p.m. (The differences in linewidth will be discussed below.)

Differences in chemical shift will also arise from more subtle differences in the nuclear environment. For example, there are two crystalline forms of silicon nitride, called α and β. Both structures consist of interleaved sheets of 8 and 12 membered rings of silicon and nitrogen. In the α form, each alternate sheet is inverted and offset slightly with respect to the underlying sheet, creating two unique silicon sites in the structure [6]. The ^{29}Si NMR spectrum of α-Si_3N_4 is given in Fig. 2. In spite of the fact that both silicon atoms are tetrahedrally surrounded by four nitrogen atoms, NMR is able to resolve them. Note that the chemical shifts are similar, reflecting the structural similarities. In the β form, the interleaved sheets of silicon and nitrogen are stacked in a regular manner. The result is that there is only one unique silicon site [7] and thus only one peak in the ^{29}Si NMR spectrum. This is also illustrated in Fig. 2. Note that the chemical shifts for α and β are similar, reflecting the similarities in nuclear environment. The average Si–N bond lengths are 0.1733 nm for the β form and 0.1747 and 0.1740 nm for the α structure [6, 7]. NMR is capable of distinguishing the silicon sites in each form even though the differences between them are very slight.

Silicon carbide (SiC), which exists in many crystalline forms, [8] provides another illustration. These forms (polytypes) are based on a cubic structure called β or a variety of hexagonal structures collectively called α. ^{29}Si NMR spectra of β-SiC and one α-SiC (6H) are given in Fig. 3. The spectra are different, reflecting the different structural environments. Similar to α-Si_3N_4, note that the ^{29}Si NMR spectrum of α-SiC (6H) contains more than one line, reflecting subtle differences in the nuclear environment. However, in this case, the three peaks have been shown to arise from differences in the second-nearest neighbour shell [9–11], roughly 0.5 nm away. This illustration reinforces the point that the "environment" is not simply the nearest neighbour network, but may involve more distant interactions, as well.

This type of sensitivity to local structure has led to many attempts [2, 12–26] to correlate chemical shift with structural details such as bond angle [12–17] and type of next-nearest neighbours [18–21]. Correlations such as these hold considerable promise for the structural analysis of amorphous materials.

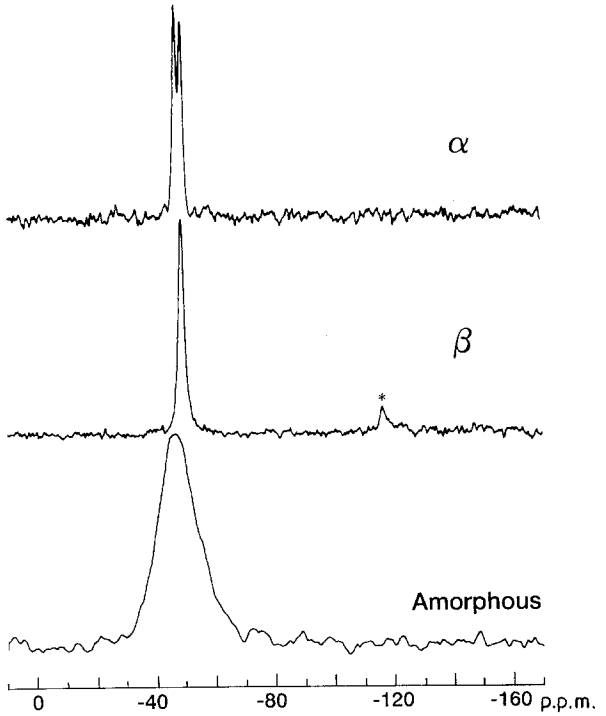

Figure 2 ^{29}Si NMR spectra of the various structural forms of silicon nitride (Si_3N_4): α and β-crystalline and amorphous (adapted, with permission, from [36]).

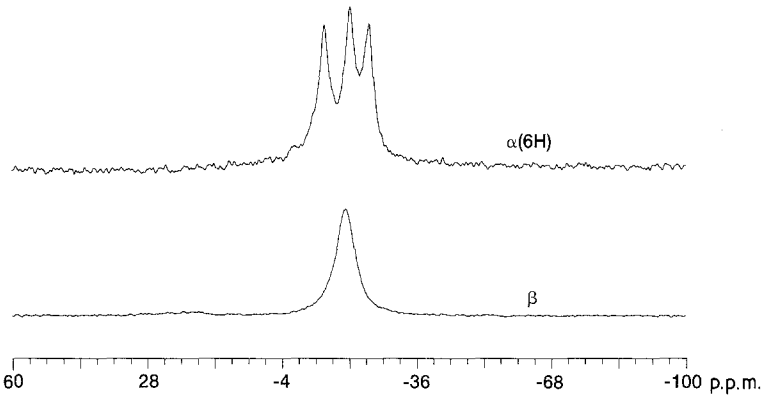

Figure 3 ^{29}Si NMR spectra of β and α (6H) silicon carbide (SiC).

3.3. Crystallinity, local order and amorphous phases

The examples above have dealt with known crystalline structures. However, NMR is *not* merely limited to systems with long range crystalline order. Instead, it observes nuclei in *any* structural environment, crystalline or amorphous. The result is that NMR has the unique ability to obtain detailed structural information on the entire composition of a system. For example, the ^{29}Si NMR spectrum of amorphous (a) silicon nitride is given in Fig. 2. The X-ray diffraction pattern of this sample revealed no crystalline features. The greater linewidth is related to heterogeneity in the local silicon environments of an amorphous phase. This can be explained by simply considering the nature of the chemical shift. For example, in β-Si_3N_4 there is one silicon site and one NMR line. In α-Si_3N_4 there are two sites and two lines. These lines have similar chemical shifts reflecting structural similarities. Thus, in an amorphous system with many diverse but similar sites, we would expect to see many lines with similar chemical shifts. The result is a series of overlapping lines, or an increase in linewidth. In other words, the observed linewidth for a given system appears to depend on, among other things, the degree of local structural order. This is illustrated for powdered and sintered α-SiC in Fig. 4. The sintered piece is expected to contain a higher degree of order at the atomic level; a fact which is reflected in the observed linewidth.

3.4. Quantitation in ceramic phases

Chemical shift and linewidth are not the only information obtained in an NMR experiment. The integrated intensity of each peak is also a sensitive indicator of structure. NMR is essentially a "counting" technique and intensities depend on the concentration of the nucleus giving rise to the NMR peak. This can provide valuable information on both specific crystal structures and on samples that are mixtures. For example, in the ^{29}Si NMR spectrum of α-Si_3N_4 (Fig. 2) there are two peaks corresponding to two crystallographically distinct sites. The integrated intensities of these peaks are in a 1 : 1 ratio, revealing that the silicon sites are also present in a 1 : 1 ratio. This can be confirmed in the crystal structure determination [6]. NMR, then, is capable of obtaining information on the number and type of each site present within a phase. Information such as this is vital for characterizing new ceramic materials and phases that are not crystallographically well defined.

Integrated NMR intensities also reveal the concentrations of components in mixtures. This is important, among other things, for quantifying the presence of impurities. For example, the ^{29}Si NMR spectrum of an amorphous Si_3N_4 with a high concentration of surface oxides is given in Fig. 5. The surface oxides appear at roughly -110 p.p.m., the chemical shift characteristic of silicon–oxygen bonds. By integrating the areas beneath the peaks we find that the surface oxides account for roughly 30% of the silicon in the sample. To turn the silicon "headcount" into a wt %, the relative formula weights of Si_3N_4 and SiO_2 must be taken into account. Correcting for the difference in the number of silicons in each structure (Si_3N_4 contributes three times as much signal as SiO_2 for equivalent numbers of formula units) indicates that the sample contains roughly 15 wt % surface oxide. This illustration emphasizes two important points: (1) NMR is

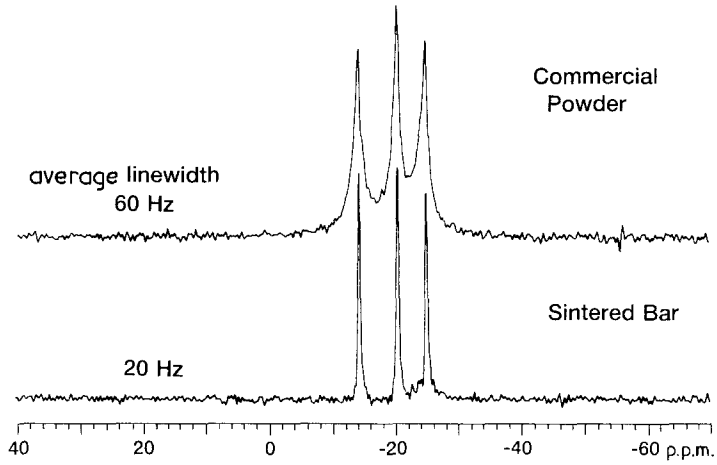

Figure 4 ^{29}Si NMR spectra of a silicon carbide (SiC) powder and sintered bar.

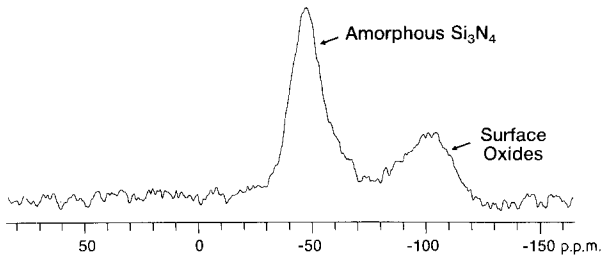

Figure 5 ^{29}Si NMR spectrum of an amorphous silicon nitride powder showing the presence of surface oxides.

capable of quantitating the various components present in a system and (2) NMR is able to quantitate *both* crystalline and amorphous phases.

In closing, it should be noted that it is necessary to use proper experimental parameters when seeking purely quantitative information. Most importantly, care must be taken to account for differences in an NMR phenomenon called "spin-lattice relaxation". The procedures for obtaining quantitative data have been well described elsewhere [1–5] and will not be repeated here.

3.5. Multinuclear NMR

All of the above illustrations have used ^{29}Si NMR, simply for introductory purposes. However, NMR is not limited to observing silicon, but is capable of studying a wide variety of nuclei [27–29]. Several examples relevant to ceramics are nitrogen (^{15}N), carbon (^{13}C), lanthanum (^{189}La), aluminium (^{27}Al) and yttrium (^{89}Y). The "observability" of these nuclei varies markedly and most work has employed ^{29}Si, ^{13}C, ^{31}P and ^{27}Al. The other nuclides have seen significantly less application, primarily because of experimental difficulties. Recently, ^{89}Y has seen application in one class of ceramic materials [30]. In most cases, the fact that NMR is multinuclear makes it possible to obtain structural information on each nuclei in each phase present in a sample. For example, we can obtain both ^{29}Si and ^{13}C NMR spectra of SiC. This is illustrated in Fig. 6. As we have previously seen, the ^{29}Si NMR spectrum of the 6H polytype reveals three types of silicon and 1 : 1 : 1 ratio. It is interesting to find that the ^{13}C NMR spectrum also reveals three types of carbon in a 1 : 1 : 1 ratio. Thus, we expect to find structural similarities between the carbons and silicons. This is, in fact, the case for the 6H polytype [10]. However, NMR reveals that the structural environments are quite different in the 15R polytype. Here, there are three silicon sites in a 1 : 2 : 2 ratio and at least five carbon sites present in a complex ratio. These ratios have been used to predict [10] the structure of the 15R polytype. Thus, NMR is capable of completely characterizing the structure of SiC. The use of this multinuclear approach can be extended to many other ceramic materials, as well.

3.6. Experimental notes

One of the primary advantages to solid-state NMR is that samples can be examined "as-received". There is no experimental preparation necessary. Samples can be powders, slips, fibres or sintered pieces. The only requirement is that the sample fit into a cylindrical holder which is roughly 20 mm in length and 10 mm in diameter. Samples larger than this are typically cut down to the appropriate size.

NMR is a bulk sensitive technique. As a result, the data obtained is representative of the entire sample under study. Results obtained by traditional methods such as vibrational spectroscopy (ATR) and X-ray diffraction (XRD) are dependent upon the "sampling depth" of the technique. The maximum sampling depth is roughly 0.5 nm for ATR and roughly 0.5 nm for XRD using typical copper radiation. In large samples where heterogeneity may exist between several microns from the surface and the interior, NMR is the method of choice. A good example of this concerns crystallization, which may occur at different rates for the surface and the interior.

4. Applications

4.1. NMR studies of lanthanum silicon nitride

Lanthanum silicon nitride ($LaSi_3N_5$) is a new type of ceramic material that is being investigated for its potential advanced heat and turbine engine applications. A structure for $LaSi_3N_5$ has been reported [31, 32]. Given in Fig. 7 is the ^{29}Si NMR spectrum of $LaSi_3N_5$ [33]. The spectrum consists of two peaks at -64.5 and -56.5 p.p.m. which are present in a 2 : 1 ratio. This indicates the presence of two "types" of silicon (as distinguished by NMR) in the sample. The spectrum is free of typical ^{29}Si impurity signals such as those for SiC and Si_3N_4. ^{13}C spectra were also acquired (not shown) and revealed that the sample was free of carbon signals. These results indicate that

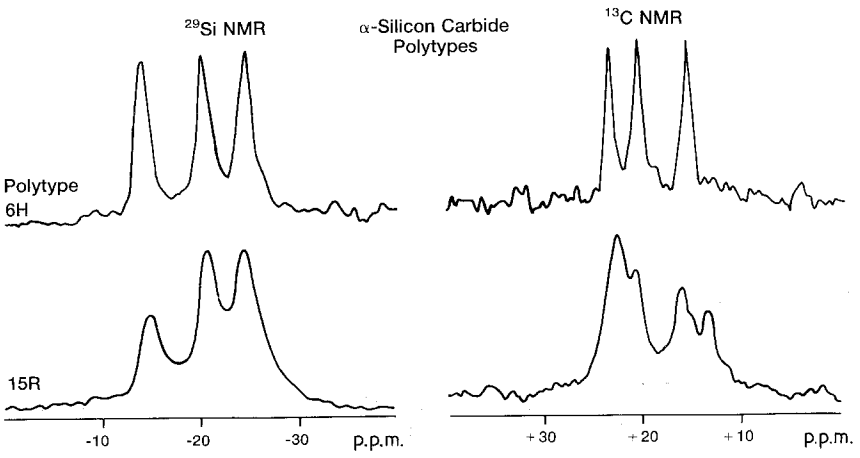

Figure 6 ^{29}Si and ^{13}C NMR spectra of two SiC polytypes (adapted, with permission, from [10]).

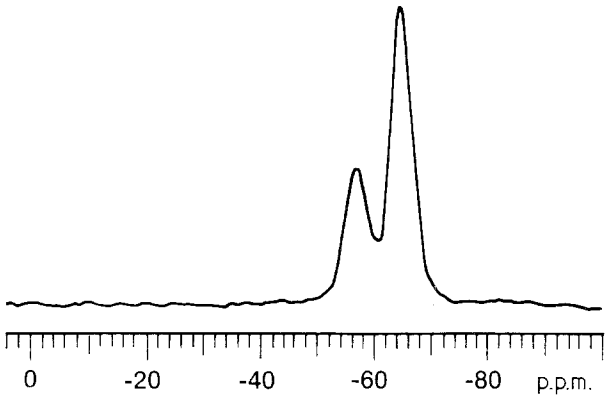

Figure 7 ^{29}Si NMR spectrum of $LaSi_3N_5$.

the sample is rather pure; a fact which has been confirmed by elemental analysis.

The observation of two ^{29}Si NMR peaks indicates the presence of two silicon types in the $LaSi_3N_5$ network. An understanding of the dominant influences affecting the chemical shift in $LaSi_3N_5$ will permit a detailed understanding of this and similar ceramic phases. In turn, this will enable one to probe the atomic level changes induced by preparation, processing and impurities.

It has been proposed [33] that the ^{29}Si NMR peaks differ in chemical shift due to the interaction between lanthanum and silicon. The nitrogens in the network do not appear to affect the shift differences since each silicon is tetrahedrally bound to four nitrogens [31, 32]. However, within a 0.5 nm sphere about silicon, there exists two types of silicon characterized by the number of neighbouring lanthanum atoms. One type, accounting for two-thirds of the total, resides in an environment with five neighbouring lanthanum atoms while the second type, accounting for the other third, has four lanthanum neighbours. These two types of silicon account for the two ^{29}Si NMR peaks. The site with four lanthanum neighbours can be assigned to the peak at -54.5 p.p.m. while the site with five lanthanum neighbours can be assigned to the -64.5 p.p.m. peak.

Studies such as this and several on SiC [9–11] suggest that a roughly 0.5 nm "sphere of influence" exists about silicon which can often be used to rationalize observed chemical shifts. This approach may prove to be valuable in other ceramic systems, as well. Changes in this "sphere", marked by changes in chemical shift, may reveal important information on the nature of atomic level interactions induced by processing, stresses and so on. For example, note that for $LaSi_3N_5$ an "increased" Si–La interaction results in a more negative chemical shift.

4.2. Determination of phase composition in silicon nitride powders

Silicon nitride (Si_3N_4) is an important ceramic, both for its own use and as starting material in the production of other ceramics and composites [34, 35]. Si_3N_4 can be present in α or β crystalline forms and in an amorphous structure. In typical Si_3N_4 precursor powders, all three phases as well as impurities such as silicon oxynitrides and silicates may be present. The physical properties of Si_3N_4 ceramics are very sensitive to the composition of the precursor powder.

For this reason, it is necessary to have a rapid, reliable method for determining the composition of batches of Si_3N_4 powder before carrying out final product formation and sintering. Traditionally, X-ray powder diffraction (XRD) has been used. However, XRD often fails in the identification of amorphous species. Recall from Fig. 2 that NMR, on the other hand, is readily capable of observing and quantifying all of the various phases of Si_3N_4.

^{29}Si NMR spectra of six Si_3N_4 powders are given in Fig. 8. All of the spectra are dominated by Si_3N_4 lines at roughly -50 p.p.m. In some samples, other silicon species such as oxynitrides and oxides are observed and can be readily identified by their chemical shift. These are also identified in Fig. 8, along with the

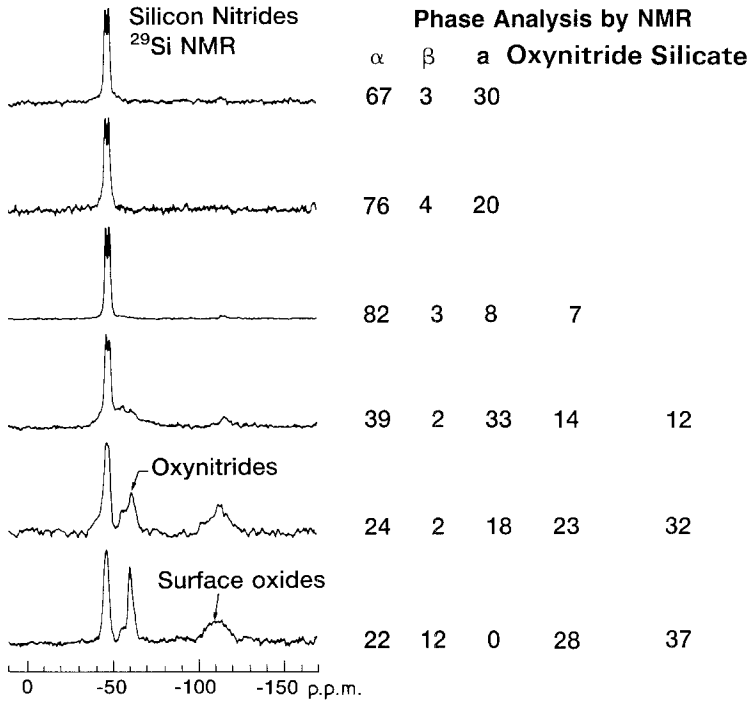

Figure 8 ^{29}Si NMR spectra of various commercial silicon nitride powders (adapted, with permission, from [36]).

results of an NMR phase composition analysis on each sample. When these values were compared with XRD analyses, it was found that as much as 30% amorphous phase was not detectable by XRD [36]. As a result, the XRD determined α/β ratio was typically 10% lower than that measured by NMR. The ability to completely and accurately characterize the phase composition of any ceramic material is an important link to understanding its physical properties.

4.3. Analysis of ceramic fibres

There has been considerable interest in the use of ceramic fibres as reinforcement in high temperature composite materials [37]. Characterization of these materials, however, is often difficult by traditional methods since they are insoluble, predominantly amorphous and often present experimental difficulties due to their sample state. Solid state NMR is being widely [38–43] used to probe these materials.

4.3.1. Survey

One method of preparing SiC fibres is by the pyrolysis of polymeric precursors. Three fibres prepared via this route have been studied by ^{29}Si NMR [40] and the results are shown in Fig. 9. The top two are standard NICALON commercial Si–C–O fibres, with the top (SGN) one containing ~15 wt% oxygen and the middle (CGN) containing ~10 wt% oxygen. In the Si–C–O fibres there are five possible tetrahedral structures for the silicon atoms if only Si–C and Si–O bonds are present (SiC_4, SiC_3O, SiC_2O_2, $SiCO_3$, and SiO_4). All appear to be present in the NICALON fibres. Oxygenated structures are more prevalent in SGN than in CGN, reflecting the higher oxygen concentration. Note that the most intense signal in both fibres occurs close to the chemical shift of SiC (−18 p.p.m.), showing SiC to be the dominant species. The bottom spectrum is of a Si–N–C fibre derived from a hydridopolysilazane polymer. Note that the spectrum of this sample is similar to that of amorphous Si_3N_4 (Fig. 2), indicating that α-Si_3N_4 is the dominant species.

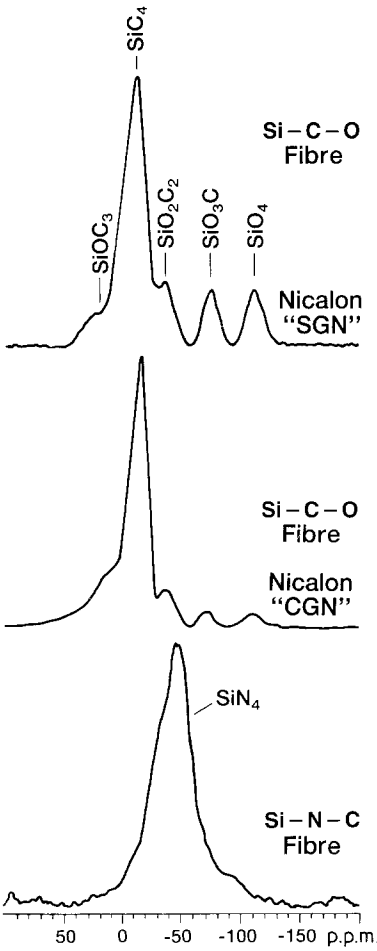

Figure 9 ^{29}Si NMR spectra of three ceramic fibres (adapted, with permission, from [40]).

4.3.2. PC precursors to SiC: Curing

Silicon carbide fibres can be prepared from a polycarbosilane precursor [38, 39]. Polycarbosilane (PC) consists of a skeleton of alternate carbon and silicon atoms. The PC fibres are obtained first by melt-spinning of PC, and then cured by heating in air at 110 to 200° C. The oxygen introduced during the oxidation curing process influences the tensile strength of the final product SiC fibres. Thus, it is important to determine the chemical structure of the oxidation-cured PC fibres and to better understand the curing process.

The ^{29}Si NMR spectrum of untreated PC fibre is given in Fig. 10. There are largely two silicon types in PC, as shown below

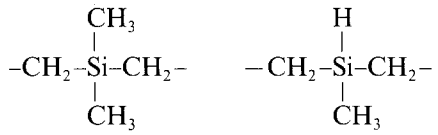

These two silicon types will hereafter be referred to as

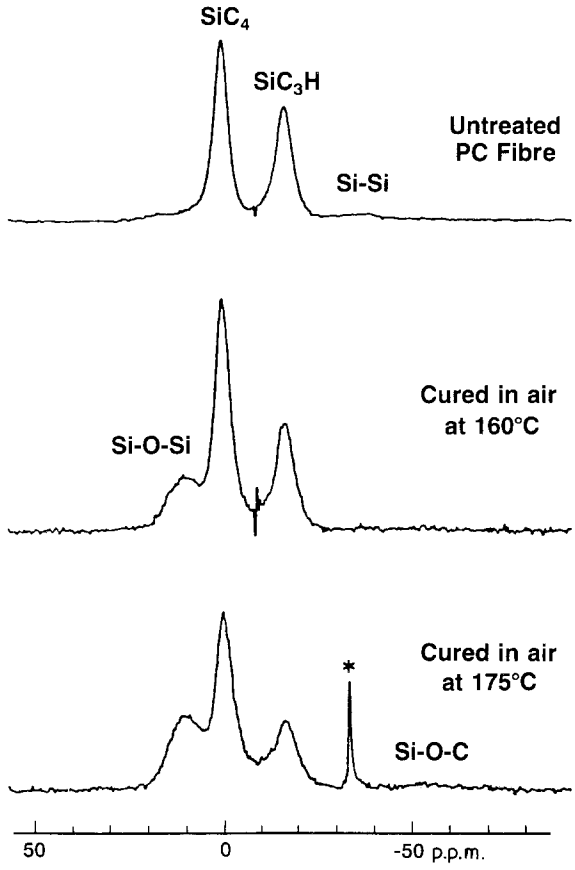

Figure 10 ^{29}Si NMR spectra of untreated and cured PC fibres (adapted, with permission, from [39]).

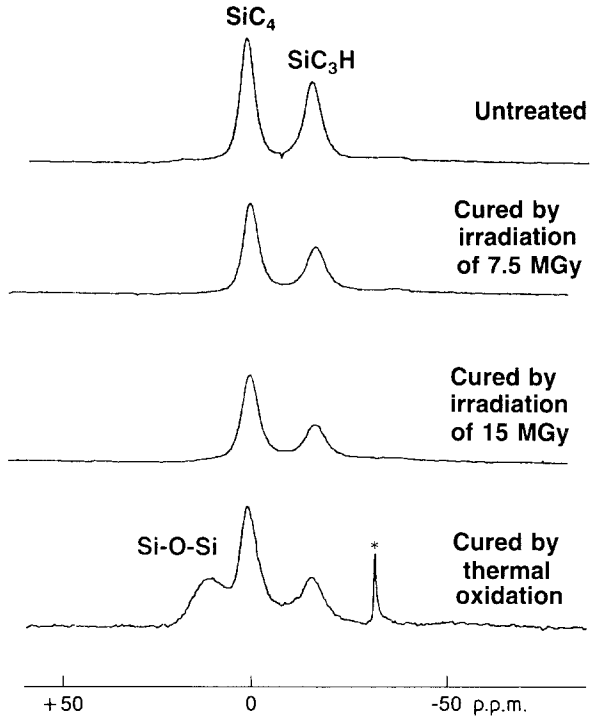

Figure 11 ^{29}Si NMR spectra of untreated and cured PC fibres (adpated, with permission, from [38]).

"SiC_4" and "SiC_3H". Assignments are indicated in the figure. The peak marked with an asterisk is due to polydimethylsilane which is used as an external reference. Spectra of PC fibres heated at 160 and 175° C in oxygen are also given. The major change observed upon curing is the formation of Si–O–Si bonds. The intensity for these bonds increases linearly with the rise of curing temperature. As the intensity of the Si–O–Si bonds increases, the intensity for "SiC_3H" decreases, indicating that the oxygen atoms attack the "SiC_3H" site and consequently convert it to an Si–O–Si bond.

As mentioned earlier, the presence of Si–O–Si bonds lowers the mechanical properties of the SiC fibre at high temperatures. In an attempt to reduce the amount of silicon oxide in the SiC fibre produced, radiation curing of the PC fibre was also investigated [38]. The ^{29}Si-NMR spectra of untreated and irradiated fibres are shown in Fig. 11. In the electron irradiation cured PC fibres, Si–O–Si signals were not observed. However, the relative intensity of the "SiC_3H" site decreased linearly with an increase in dose. This indicates that the Si–H bond is broken by the electron irradiation and that an Si–C or Si–Si bond, is formed.

4.4. An NMR investigation of dispersion aid mechanisms

Many ceramic powders do not sinter well due to heterogeneities such as particle size distribution and uneven dispersion. One approach in solving this problem has been to suspend the powder in a slurry containing a "dispersion aid" (DA). These DA's typically contain a long chain hydrophobic moiety and a reactive site which will "couple" with the inorganic solid. In concept, the DA then forms a long chain monomolecular layer around each particle, thereby improving dispersion. This is illustrated in Fig. 12. When the solution is removed from the slurry, the DA acts to prevent phase separation, promote adhesion and create a more uniformly dispersed ceramic. This typically results in improved physical and mechanical properties such as rheology and impact strength. An understanding of the interaction between the DA and the ceramic particle is vital for optimizing these properties. NMR is uniquely capable of studying the DA in solution, as part of a slurry and as a solid within the ceramic network.

In this illustration, ^{31}P NMR is used to follow the interaction between zirconia powder and a titanate–polyphosphate DA reported to have the following structure

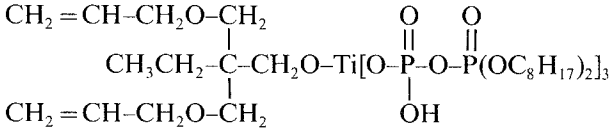

The ^{31}P NMR spectrum of the dispersion aid in water is given in Fig. 13 (bottom). This spectrum, acquired using standard solution state NMR methods [44] (including proton decoupling), contains many ^{31}P peaks which indicates the presence of many ^{31}P moieties. This result is inconsistent with the proposed single structure provided by the supplier. In fact, the spectrum is consistent with partial polymerization into a mixture of polyphosphates and both linear, branching and ring structures [45]. FAB-MS studies are in agreement with

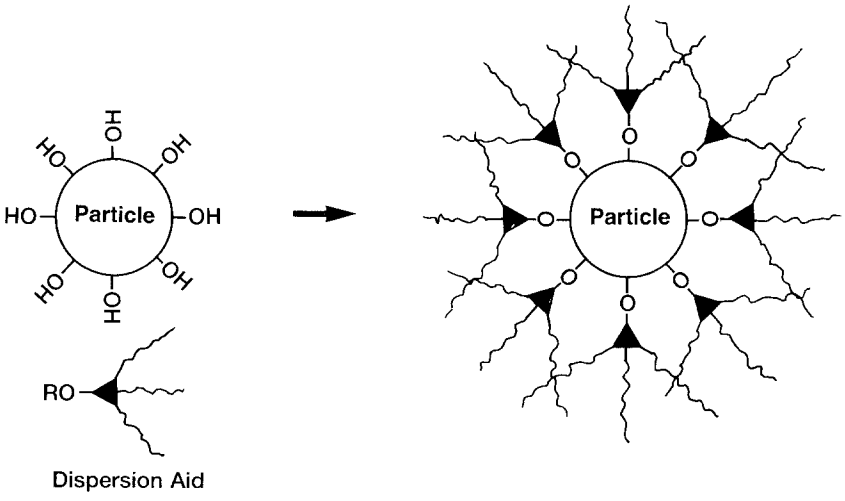

Figure 12 Schematic illustration of the dispersion aid–ceramic particle interaction.

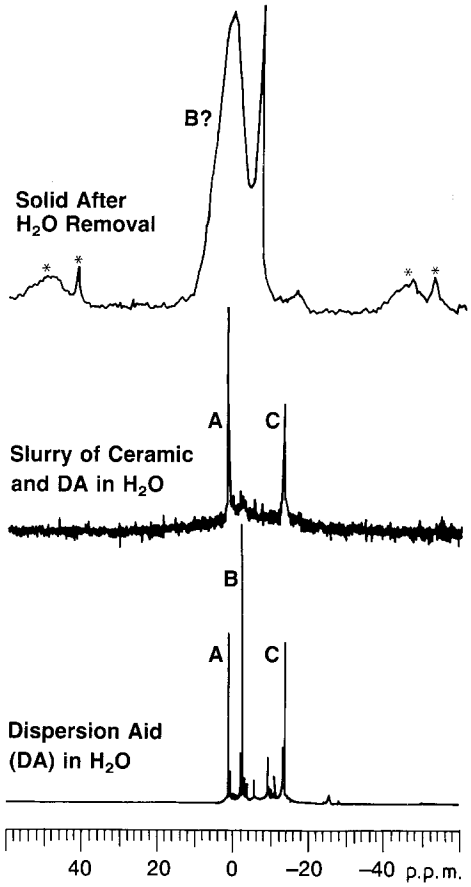

Figure 13 ^{31}P NMR spectra of a dispersion aid as a solution, a slurry and a solid (see text).

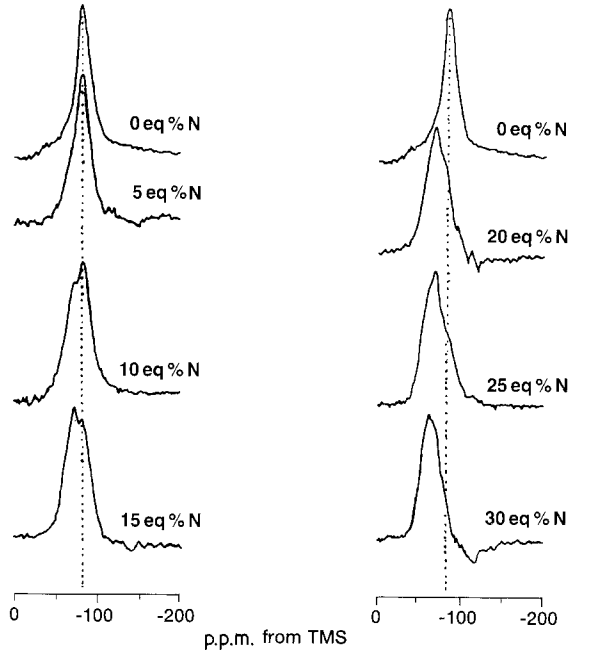

Figure 14 ^{29}Si NMR spectra of a series of Y–Si–Al(O, N) glasses with increasing substitution of nitrogen for oxygen (adapted, with permission, from [46]).

the NMR that the solution, as received, is a mixture of polyphosphate components.

A complete characterization of the DA is underway. However, even without this information, several interesting points can be observed from Fig. 13. The spectrum of the DA is dominated by three major ^{31}P lines (A, B, C), indicating three major "types" of ^{31}P sites. When the DA is suspended in a slurry with the ceramic, two of these peaks (A, C) remain while the third (B) is significantly reduced. Without definitive assignments, it is difficult to interpret this observation. However, one might speculate that the ^{31}P site which gives rise to peak B is now bound to the solid ceramic surface and cannot be "seen" by traditional solution state NMR. When the water is removed from the slurry, a solid mixture of ceramic and DA remains which can be studied by solid state ^{31}P NMR (employing high power proton decoupling [1–5]). In the spectrum of the solid material (top, Fig. 13), peaks marked with an asterisk are due to spectral features called spinning sidebands and should be ignored. The ^{31}P spectrum of the solid is dominated by two signals, one sharp and one broad. Again, without a detailed structure determination and spectral assignment it is difficult to interpret this result. However, one might speculate that the broad line is due to B bound to the ceramic and that the narrow line is due to "free" B in the network.

The results shown here are clearly preliminary and the interpretation speculative. However, this study demonstrates, for the first time, the ability of NMR to study the dispersion aid in each of its states and to characterize the DA-ceramic interaction.

4.5 Structure of SiAlON ceramics

"SiAlON" ceramics are materials composed of three-dimensional arrangements of (Si, Al)(O, N)$_4$ tetrahedra and occasionally contain aluminium in a six fold octahedral coordination. These ceramics are of interest because of their thermal and mechanical properties. Properties such as the glass transition temperature, hardness and elastic modulus are dependent on the substitution of nitrogen for oxygen in the local structure of oxynitride glasses. However, the structure of many of these phases remains unknown. Direct evidence for the incorporation of nitrogen in the network is sparse and there is no direct evidence of aluminium–nitrogen bonding. Traditional X-ray diffraction methods have been hampered by similar X-ray scattering factors for aluminium and silicon. Solid state NMR, however, is providing a new and powerful method for probing the structure and chemistry of these materials [46–53].

For example, consider a series of Y–Si–Al–(O, N) glasses of increasing nitrogen content. ^{29}Si NMR spectra of several SiAlON materials with constant Y : Si : Al ratio and increasing substitution of nitrogen for oxygen are given in Fig. 14. NMR is capable of identifying the discrete (Si, Al)(O, N)$_4$ structural units in these materials. Each spectrum is composed of several partially resolved peaks, indicating the coexistence of a variety of Si(O, N)$_4$ structural groups. A detailed characterization of the shifts is presented elsewhere [46]. However, it can be said that the observed spectra are consistent with the occurrence of Si(O$_3$N) and Si(O$_2$N$_2$) groups together in the network. Note that with increasing nitrogen substitution, there is a progressive shift in intensity that can be explained as nitrogen progressively entering the network in a three-fold coordination bonding to two silicon and one

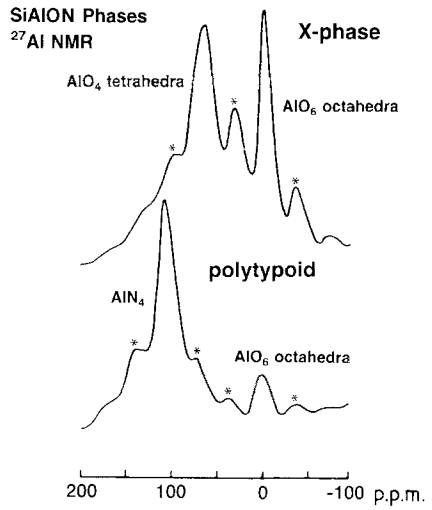

Figure 15 ^{27}Al NMR spectra of SiAlON X-phase and polytypoid (adapted, with permission, from [47]).

aluminium atom. The data obtained also reveal a preference for Si–N bonding compared with Al–N bonding.

^{27}Al NMR has also been used to study SiAlON systems. Fig. 15 shows the ^{27}Al NMR spectra of two SiAlONs referred to as "X-phase" and as a "polytypoid" [47]. The signals attributed to octahedral AlO_6 and tetrahedral AlO_4 and AlN_4 are indicated. Peaks marked with an asterisk are due to spinning sidebands and can be ignored. For the x-phase, the observed 1.9 : 1.0 intensity ratio of tetrahedral : octahedral aluminium is in complete agreement with the structure, which provides for 20 to 22 tetrahedral and 12 octahedral aluminium atoms per unit cell. The spectrum of the polytypoid indicates the presence of only two types of aluminium. The small signal at 2.3 p.p.m. is unambiguously attributed to AlO_6 octahedra and the intense signal at 108.2 p.p.m. is tentatively assigned to aluminium coordinated by four nitrogen atoms. The intensity ratio of the two signals is 9 : 1. The results of this preliminary examination show that NMR can readily and quantitatively distinguish the various types of aluminium in complex oxynitride ceramics.

4.6. Sintering of Si_3N_4 and "grain boundary phases"

The densification process used to turn Si_3N_4 powders into structural ceramics is called sintering. In this process, the precursor powder is heated in the absence of oxygen and often under high pressure, converting α-Si_3N_4 into β-Si_3N_4. Since pure Si_3N_4 will not sinter, this process is often performed by mixing α-Si_3N_4 powder with 5 to 10% of a sintering aid. One common aid is Y_2O_3. A small amount of the powder reacts with the sintering aid to form new compounds that tend to collect on the grain boundaries between microcrystals of β-Si_3N_4. These intergranular phases have important consequences on physical and thermal properties of Si_3N_4 components and thus need to be identified and quantified. Here, ^{29}Si MAS NMR is used to detect, identify, and quantify Y–Si–O–N phases associated with the grain boundaries [54]. It should be noted that NMR is capable of observing these phases but cannot distinguish them from similar phases which may be

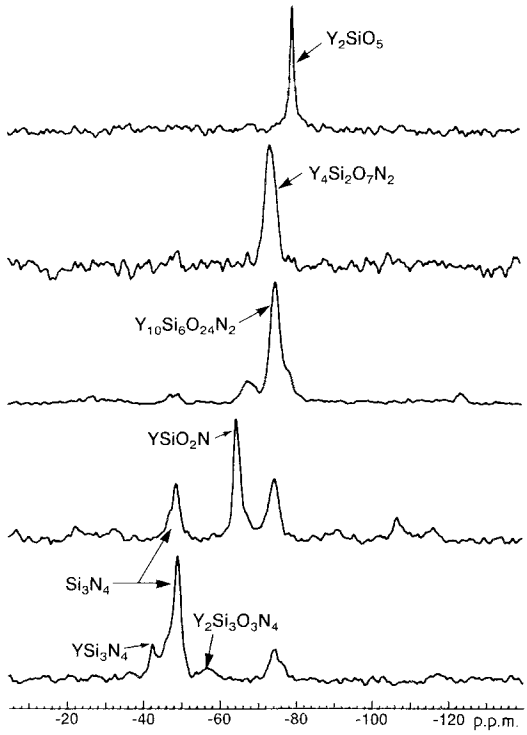

Figure 16 ^{29}Si NMR spectra of potential grain boundary phases which occur upon sintering Si_3N_4 with Y_2O_3.

present in other parts of the sample. It has been previously shown that the major source of Y–Si–O–N phase impurity is at the grain boundary of these sintered ceramics. Thus, the assumption is made that the NMR signals are due to phases at the grain boundaries.

The ^{29}Si MAS NMR spectra of potential grain boundary phases are given in Fig. 16. Only the spectra of Y_2SiO_5 and $Y_4Si_2O_7N_2$ show pure materials. All of the other samples consist of mixtures of the phases. The resonance frequencies of these materials are well resolved, permitting ready identification in the sintered solid [54, 55].

^{29}Si NMR spectra of two sintered Si_3N_4 samples are given in Fig. 17. In agreement with the known conversion of α to β during sintering, the similarity between the spectra of ceramics A and B with the β powder in Fig. 2 is not surprising. The linewidth is narrowed from 150 Hz for the powder to 116 Hz for the ceramic, reflecting an increase in local order as discussed earlier. For ceramic B, a shoulder indicating the presence of some α-Si_3N_4 is just visible. Note the presence of phases associated with the grain boundaries in both ceramics. The intergranular Y–Si–O–N compounds produce less intense features due to their lower relative concentration and are expanded in the figure. Integration of these peaks permits determination of the wt % of these phases and the results are listed below.

Ceramic	α-Si_3N_4	β-Si_3N_4	$YSiO_2N$	$Y_{10}Si_6O_{24}N_2$
A	30.5	64.8	4.7	–
B	–	87.8	–	12.2

For Sample B, the determined percentage of Y–Si–O–N phase is virtually identical to the theoretical wt % of 12.9%. However, in Sample A, the determined 4.7% is significantly less than the expected 14.4% based on

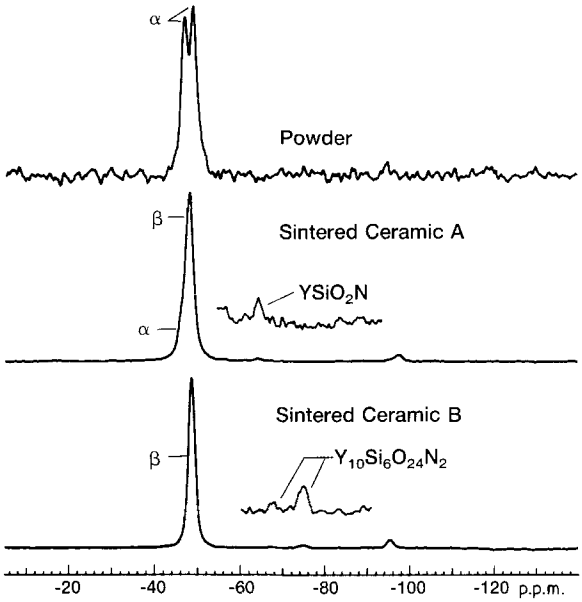

Figure 17 ^{29}Si NMR spectra of a Si_3N_4 powder and two sintered pieces.

stoichiometry. This discrepancy may be simply related to the method of quantitation used and further work is planned.

In the sintering of many ceramics, subtle differences in the intergranular phases have a profound effect on the physical properties. Techniques capable of non-destructively identifying and quantifying these phases are crucial. NMR provides an important and powerful tool for probing solid state chemistry in these systems.

4.7. Unusual spinning sideband observations

It was noted several times throughout the text that in some spectra, features called "spinning sidebands (SSB)" were present that should be ignored. Adequate explanations for the appearance of SSB's are neither trivial nor within the scope of this section. However, it can be said that they are a direct result of the fact that the sample is rotated during data acquisition. It can also be said that for a given rotation speed, the relative intensity of an SSB is related to the local "anisotropy" about the given nucleus. Unfortunately, "anisotropy" can take on many meanings including electron distribution, bonding and so on.

We have observed that in silicon carbide (SiC) powders, the appearance of SSB's is sample dependent. Typical examples of this can be seen in Fig. 18 for two commercially available β-SiC powders. The peak marked with an arrow is due to the central (isotropic) resonance for β-SiC and peaks marked with an asterisk are due to SSBs. According to the manufacturer the only difference between the samples is particle size distribution and average particle size. However, NMR is sensitive to the nuclear environment, which is orders of magnitude smaller than the particle size. XRD studies failed to detect any difference between the samples. Preliminary EPR investigations, on the other hand, appear to have identified a correlation between the appearance of SSBs and the concentration of paramagnetic centres [56], a phenomenon that has been reported previously [57]. We have also observed that processing can have a dramatic effect on the intensity of the SSBs. Future investigations on the nature of these effects may provide new clues into the atomic level changes that take place during processing.

Acknowledgements

For the examples taken directly from the literature, the original research groups are acknowledged. The work on $LaSi_3N_5$ was done in collaboration with J. Yamanis and B. Li. The preliminary dispersion aid/ceramic study was done in collaboration with A. Fanelli. Finally, we would like to thank R. D. Sedgwick and R. O. Carter III for their continued support of this work.

References

1. C. A. FYFE, "Solid-State NMR for Chemists" (CFC Press, Guelph, 1983).
2. E. OLDFIELD and R. J. KIRKPATRICK, *Science* **227** (1985) 1537.
3. G. E. MACIEL, *Science* **226** (1984) 282.
4. E. FUKUSHIMA and S. B. W. ROEDER, "Experimental Pulse NMR" (Addison-Wesley, London, 1981).

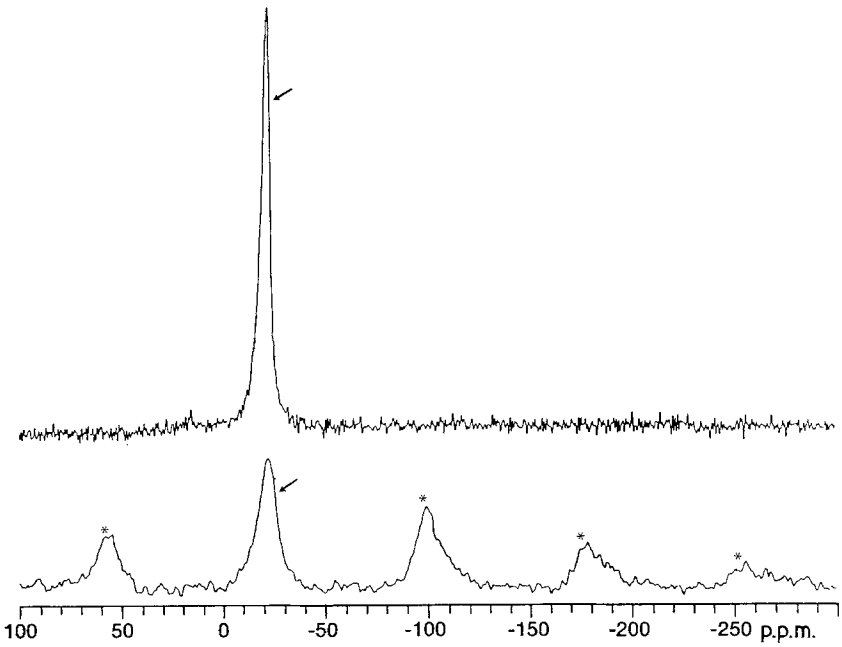

Figure 18 ^{29}Si NMR spectra of two commercially available β-SiC powders.

5. M. MEHRING, "Principles of High Resolution NMR in Solids" (Springer, New York, 1983).
6. K. KATO, Z. INOUE, K. KIJIMA, I. KAWADA, H. TANAKA and T. YAMANE, *J. Amer. Ceram. Soc.* **58** (1975) 90.
7. R. GRUN, *Acta Crystallogr.* **B35** (1979) 800.
8. R. C. MARSHALL, J. W. FAUST and C. E. RYAN, "Silicon Carbide" (University of South Carolina Press, Columbia, 1973).
9. G. R. FINLAY, J. S. HARTMAN, M. F. RICHARDSON and B. L. WILLIAMS, *J. Chem. Soc., Chem. Commun.* (1985) 159.
10. J. S. HARTMAN, M. F. RICHARDSON, B. L. SHERRIFF and B. G. WINSBORROW, *J. Amer. Chem. Soc.* **109** (1987) 6059.
11. J. R. GUTH and W. T. PETUSKEY, *J. Phys. Chem.* **91** (1987) 5361.
12. J. V. SMITH and C. S. BLACKWELL, *Nature* **303** (1983) 223.
13. A. R. GRIMMER, F. VON LAMPE, M. MAGI and E. LIPPMAA, *Mh. Chem.* **114** (1983) 1053, **115** (1984) 561.
14. G. ENGELHARDT and R. RADEGLIA, *Chem. Phys. Lett.* **108** (1984) 271.
15. R. RADEGLIA and G. ENGELHARDT, *Chem. Phys. Lett.* **114** (1985) 28.
16. S. RAMDAS and J. KLINOWSKI, *Nature* **308** (1984) 521.
17. N. JANES and E. OLDFIELD, *J. Amer. Chem. Soc.* **107** (1985) 6769.
18. E. LIPPMAA, M. MAGI, A. SAMOSON, G. ENGELHARDT and A. R. GRIMMER, *ibid.* **102** (1980) 4889.
19. E. LIPPMAA, M. MAGI, A. SAMOSON, M. TARMAK and G. ENGELHARDT, *ibid.* **103** (1981) 4992.
20. A. R. GRIMMER, *Chem. Phys. Lett.* **119** (1985) 416.
21. M. MAGI, E. LIPPMAA, A. SAMOSON, G. ENGELHARDT and A. R. GRIMMER, *J. Phys. Chem.* **88** (1984) 1518.
22. B. L. SHERRIFF and H. D. GRUNDY, *Nature* **332** (1988) 819.
23. K. A. SMITH, R. J. KIRKPATRICK, E. OLDFIELD and D. M. HENDERSON, *Amer. Miner.* **68** (1983) 1206.
24. A. R. GRIMMER and R. RADEGLIA, *Chem. Phys. Lett.* **106** (1984) 262.
25. J. M. NEWSAM, *J. Phys. Chem.* **89** (1985) 2002.
26. J. B. HIGGINS and D. E. WOESSNER, *Eos* **63** (1982) 1139.
27. J. MASON, "Multinuclear NMR" (Plenum, New York, 1984).
28. R. K. HARRIS and B. E. MANN, "NMR and the Periodic Table" (Academic, New York, 1978).
29. T. AXENROD and G. A. WEBB, "Nuclear Magnetic Resonance Spectroscopy of Nuclei Other Than Protons" (Wiley, New York, 1974).
30. R. DUPREE and M. E. SMITH, *Chem. Phys. Lett.* **148** (1988) 41.
31. Z. INOUE, *J. Mater. Sci. Lett.* **4** (1985) 656.
32. Z. INOUE, M. MITOMO and N. II, *J. Mater. Sci.* **15** (1980) 2915.
33. J. YAMANIS, G. HATFIELD, W. HAMMOND, B. LI and F. REIDINGER, submitted.
34. T. G. KALAMASZ, G. GOTH, R. P. WORTHEN and A. E. PASTO, *Automotive Engng* **96** (1988) 63.
35. M. G. MILBERG, *Chemtech* **17** (1987) 552.
36. K. R. CARDUNER, R. O. CARTER, M. E. MILBERG and G. M. CROSBIE, *Anal. Chem.* **59** (1987) 2794.
37. H. W. RAUCH, W. H. SUTTON and L. R. McCREIGHT, "Ceramic Fibers and Fibrous Composite Materials" (Academic, New York, 1968).
38. T. TAKI, K. OKAMURA, M. SATO, T. SEQUCHI and S. KAWANISHI, *J. Mater. Sci. Lett.* **7** (1988) 209.
39. T. TAKI, S. MAEDA, K. OKAMURA, M. SATO and T. MATSUZAWA, *ibid.* **6** (1987) 826.
40. J. LIPOWITZ and G. L. TURNER, *Polym. Prepr.* **29** (1988) 74.
41. K. E. INKNOTT, S. M. WHARRY and D. J. O'DONNELL, *Mater. Res. Soc. Symp. Proc.* **73** (1986) 165.
42. J. LIPOWITZ, J. A. RAHE and T. M. CARR, *ACS Symp. Ser.* **360** (1988) 156.
43. R. WEST and J. MAXKA, *ibid.* **360** (1988) 6.
44. C. H. YODER and C. D. SCHAEFFER, "Introduction to Multinuclear NMR" (Benjamin/Cummings, Menlo Park, 1987).
45. M. VILLA, K. R. CARDUNER and G. CHIODELLI, *J. Solid State Chem.* **69** (1987) 19.
46. R. S. AUJLA, G. LENG-WARD, M. H. LEWIS, E. F. W. SEYMOUR, G. A. STYLES and G. W. WEST, *Phil. Mag.* **B54** (1986) L51.
47. J. KLINOWSKI, J. M. THOMAS, D. P. THOMPSON, P. KORGUL, K. H. JACK, C. A. FYFE and G. C. GOBBI, *Polyhedron* **3** (1984) 1267.
48. N. D. BUTLER, R. DUPREE and M. H. LEWIS, *J. Mater. Sci. Lett.* **3** (1984) 469.
49. B. C. GERSTEIN and A. T. NICOL, *J. Non-Cryst. Solids* **75** (1985) 423.
50. R. DUPREE, M. H. LEWIS, G. LENG-WARD and D. S. WILLIAMS, *J. Mater. Sci. Lett.* **4** (1985) 393.
51. K. A. SMITH, R. J. KIRKPATRICK, E. OLDFIELD and D. M. HENDERSON, *Amer. Mineral.* **68** (1983) 1206.
52. R. DUPREE, M. H. LEWIS and M. E. SMITH, *J. Amer. Chem. Soc.* **110** (1988) 1083.
53. *Idem, J. Appl. Crystallogr.* **21** (1988) 109.
54. K. R. CARDUNER, R. O. CARTER, M. J. ROKOSZ, G. M. CROSBIE and E. D. STILES, *Chem. Mater* **1** (1989) 302.
55. R. DUPREE, M. H. LEWIS and M. E. SMITH, *J. Amer. Chem. Soc.* **60** (1988) 249.
56. K. R. CARDUNER, J. L. GERLOCK and G. HATFIELD, in progress.
57. E. OLDFIELD, R. A. KINSEY, K. A. SMITH, J. A. NICHOLS and R. J. KIRKPATRICK, *J. Magn. Reson.* **51** (1983) 325.

Received 23 January
and accepted 13 February 1989